ACS APPLIED MATERIALS & INTERFACES

Research Article

www.acsami.org

Layer-by-Layer TiO_2/WO_3 Thin Films As Efficient Photocatalytic Self-Cleaning Surfaces

Antonio Otavio T. Patrocinio,*[,†] Leonardo F. Paula,[†] Roberto M. Paniago,[‡] Janna Freitag,[§] and Detlef W. Bahnemann*[,§]

[†]Instituto de Química, Universidade Federal de Uberlandia, Uberlândia, Minas Gerais 38400-902 Brazil

[‡]Instituto de Ciências Exatas, Universidade Federal de Minas Gerais, Belo Horizonte, Minas Gerais 31270-901, Brazil

[§]Leibniz Universität Hannover, Institut für Technische Chemie, Photocatalysis and Nanotechnology, Callinstrasse 3, D-30167 Hannover, Germany

Supporting Information

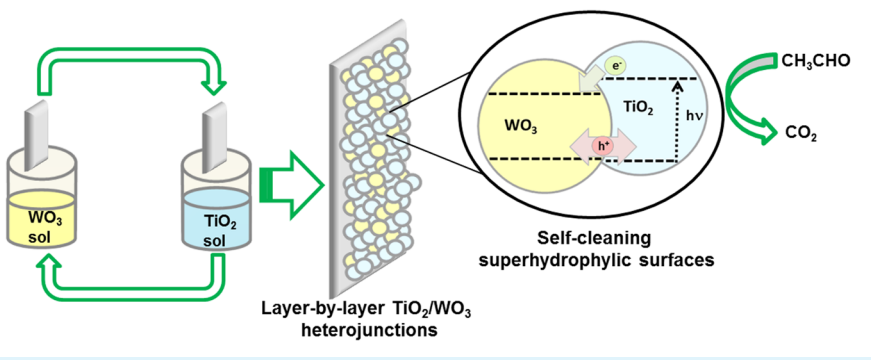

ABSTRACT: New TiO_2/WO_3 films were produced by the layer-by-layer (LbL) technique and successfully applied as self-cleaning photocatalytic surfaces. The films were deposited on fluorine doped tin oxide (FTO) glass substrates from the respective metal oxide nanoparticles obtained by the sol−gel method. Thirty alternative immersions in pH = 2 TiO_2 and pH = 10 WO_3 sols resulted in ca. 400 nm thick films that exhibited a W(VI)/Ti(IV) molar ratio of 0.5, as determined by X-ray photoelectron spectroscopy. Scanning electron microscopy, along with atomic force images, showed that the resulting layers are constituted by aggregates of very small nanoparticles (<20 nm) and exhibited nanoporous and homogeneous morphology. The electronic and optical properties of the films were investigated by UV−vis spectrophotometry and ultraviolet photoelectron spectroscopy. The films behave as nanoscale heterojunctions, and the presence of WO_3 nanoparticles caused a decrease in the optical band gap of the bilayers compared to that of pure LbL TiO_2 films. The TiO_2/WO_3 thin films exhibited high hydrophilicity, which is enhanced after exposition to UV light, and they can efficiently oxidize gaseous acetaldehyde under UV(A) irradiation. Photonic efficiencies of ξ = 1.5% were determined for films constituted by 30 TiO_2/WO_3 bilayers in the presence of 1 ppm of acetaldehyde, which are ∼2 times higher than those observed for pure LbL TiO_2 films. Therefore, these films can act as efficient and cost-effective layers for self-cleaning, antifogging applications.

KEYWORDS: *self-cleaning, metal oxides films, layer-by-layer, TiO_2/WO_3 films, photocatalysis*

INTRODUCTION

Photoinduced (super)hydrophilic properties of TiO_2 films have been extensively studied,[1−10] since they were first observed by Wang and co-workers.[11] These films can be directly applied as antifogging surfaces in building facades, windows, vehicles, clothes, and so on.[12−15] Although the mechanism of this phenomenon is still under investigation, commercial products such as Pilkington Activ self-cleaning glass are already available.[16−18]

Intense research efforts have been spent to improve the mechanical and photocatalytic properties of TiO_2-based films for self-cleaning applications. For example, several authors have reported TiO_2 films doped with anions or transitions metals, which lead to better photonic efficiencies and visible-light activity.[19−24] Another interesting approach to enhance the self-cleaning properties is the preparation of mixed metal oxide films.[25−29] TiO_2/SiO_2 films on polycarbonate have been successfully employed as hydrophilic surfaces with better adhesion than bare TiO_2 films. Miyauchi et al. reported TiO_2/WO_3 films deposited by a spin-coating method that exhibited high hydrophilic properties after UV irradiation with intensities as low as 1 μW cm^{-2}.[30]

Received: July 1, 2014
Accepted: September 12, 2014
Published: September 12, 2014

The great wettability of TiO_2/WO_3 heterostructures has called particular attention and is attributed to the enhanced electron−hole separation efficiency in relation to bare TiO_2 films.[31−35] In the TiO_2/WO_3 heterojunctions, photogenerated electrons are transferred from TiO_2 to WO_3, while holes are transferred in the opposite direction in the valence band, decreasing the charge recombination rate. As a result, interesting photochromic and photocatalytic properties are observed.

Different authors have reported the influence of morphologic properties and the W(VI)/Ti(IV) ratio on the photoelectrochemical properties of TiO_2/WO_3 films.[36−38] It was observed that low W(VI)/Ti(IV) ratios enhance the photocatalytic activity toward oxidation of organic pollutants. As the tungsten content is increased, the films start to exhibit photochromic properties and the photocatalytic activity decreases significantly.[39] The deposition process also plays a role on the photoelectrochemical behavior of the films, as shown by Irie and co-workers.[40]

In this work, we have employed the layer-by-layer (LbL) technique followed by a heating post-treatment to prepare TiO_2/WO_3 nanoparticulate films with suitable optical, electronic, and photocatalytic properties for application as self-cleaning surfaces. LbL is a promising up-scalable method used to achieve high-quality, solution-processed films.[41−45] It is based on the self-assembly growth of films in a substrate due to attraction forces (generally electrostatic) between different species. The main advantage of LbL assembly is the production of uniform thin films with precise morphological, compositional, and thickness control. To evaluate the photocatalytic properties of the TiO_2/WO_3 LbL films, we employed the acetaldehyde (CH_3CHO) photodegradation test, according to ISO standard 22197-2.[46] Acetaldehyde is one of the principal indoor air pollutants and one of the most abundant carbonyl compounds in the atmosphere. Thus, it is of great interest to degrade acetaldehyde in an environmentally compatible reaction.[47]

EXPERIMENTAL SECTION

All chemicals were analytical or high-performance liquid chromatography (HPLC) grade and were used as received. Positively charged TiO_2 nanoparticles were prepared by hydrolysis of titanium(IV) isopropoxide (Aldrich, 97%) in a 1 mol L^{-1} HNO_3 aqueous solution, as previously reported.[48] The concentration of the resulting sol was adjusted to 10 mg mL^{-1} (pH = 2). Negatively charged tungsten species were obtained through hydrolysis of $Na_2WO_4{\cdot}2H_2O$ (Aldrich) under alkaline conditions. Then, 750 mg of sodium tungstate were added to 60.0 mL of pH = 10 NH_4OH/NH_4Cl buffer. The solution was kept under stirring for 36 h at room temperature to yield a stable translucid yellowish sol.

TiO_2/WO_3 films were deposited onto cleaned fluorine doped tin oxide (FTO) substrates (Pilkington, TEC-15) by the LbL technique, in which the substrate is alternatively immersed for 3 min in TiO_2 (pH = 2) or WO_3 (pH = 10) sols. After each immersion, the substrate was rinsed with reagent-grade water (30 s, under magnetic stirring) and dried with compressed air. In this study, 30 bilayers were deposited on FTO surface. The dried films were sintered at 450 °C to ensure mechanical stability. To better evaluate the effect of WO_3 nanoparticles on the electronic and photocatalytic properties, we also prepared LbL films with only TiO_2 nanoparticles by alternatively immersions of the substrates on TiO_2 sols at pH = 2 and 10. Further details about the preparation of pure LbL TiO_2/TiO_2 bilayers can be found elsewhere.[49]

The LbL films were characterized by X-ray diffraction (XRD) analysis using an XRD600 powder diffractometer (Shimadzu) operating at 40 kV and 30 mA employing Cu Kα radiation. The diffractograms were collected in the 20−90° range with 0.02° steps. Raman spectroscopy was performed in a confocal Horiba Jobin Yvon T64000 Raman system. Samples were excited at 633 nm (delivered by a He−Ne laser), and the scattered light was collected at back scattering configuration employing a 20× objective lens. All Raman measurements were performed at room temperature.

The film morphologies were evaluated by field-emission scanning electron microscopy (FESEM) using a JSM 7401F (JEOL) microscope and by atomic force microscopy (AFM) using a SPM-9600 scanning probe microscope (Shimadzu). AFM images were registered under contact mode at a scan rate of 1 Hz. The thicknesses of the LbL films were determined by perfilometry using a P-16 Stylus profilometer (KLA Tencor). X-ray photoelectron spectroscopy experiments were carried out using an ESCALAB 220ixL spectrometer (VG Scientific) equipped with a hemispherical electron energy analyzer and using Mg Kα radiation ($h\nu$ = 1487 eV), as previously reported.[48] The binding energies were measured using the C 1s peak at 284.6 eV as internal reference. Ultraviolet photoelectron spectroscopy (UPS) has been employed for valence band investigations using the same ESCALAB electron analyzer. Measurements were performed at 2 eV pass energy using He I photons ($h\nu$ = 21.22 eV) from a differential pumped discharge lamp.

The optical properties of the TiO_2/WO_3 films were evaluated by UV−vis spectroscopy using a Shimadzu UV-2501 BC spectrometer employing a blank FTO as reference. Diffuse reflectance spectra were acquired using a Varian Cary 100 equipped with an integration sphere. $BaSO_4$ was used as a non-absorbing reference.

Photo-oxidation of CH_3CHO was carried out in an experimental setup consisting of a gas supply, three mass flow controllers, a humidifier, a photoreactor made of poly(methyl methacrylate) (PMMA) and covered with a borosilicate glass, and a Syntech Spectras GC 955 gas chromatograph, as described previously.[50] The active area of the samples was 5 cm^2. All samples were precleaned under UV-irradiation (10 W/m^2, 365 nm) prior to photocatalytic tests. The gaseous reaction mixture was prepared by mixing streams of dry air (500 mL/min), wet air (500 mL/min, relative humidity of 50%), and 10 or 50% of CH_3CHO/N_2 mixture (approximately 50 mL/min) to obtain a final CH_3CHO concentration at 297 K of 1 or 5 ppm, respectively. The photoreactor was illuminated by four UVA lamps (Philips CLEO 15 W) at 1 mW cm^{-2}. Prior to the photocatalytic tests, the photoreactor was purged with the CH_3CHO/water vapor/air mixture without illumination until a steady CH_3CHO concentration be achieved at the outlet. Afterward, the sample was irradiated for approximately 120 min.

Photonic efficiency (ξ), which is defined as the ratio of the degradation rate of CH_3CHO and the incident photon flux was calculated as described elsewhere[50] by using eq 1, in which h is the Planck constant, c is the light velocity, N_A is the Avogadro's number, Δn is the difference of the steady state acetaldehyde concentration in the dark (n_{dark}) and under irradiation (n_{light}), $\dot{V}$ is the volume flux (m^3 s^{-1}), R is the gas constant, T is the temperature, ϕ is the light intensity, S is the illuminated area, and λ is the irradiation wavelength (350 nm). For the calculations, it was considered the fraction of light absorbed by the samples ($1-10^{-A}$) is taken into account, in which A is the absorbance of the film at 350 nm. The maximum theoretical photonic efficiencies (ξ_{th}) under these conditions are 4.7 and 23.5%, respectively, for initial CH_3CHO concentrations of 1 and 5 ppm.

$$\xi = \frac{hcN_A \Delta n \dot{V}}{\phi SRT\lambda(1 - 10^{-A})} \quad (1)$$

RESULTS AND DISCUSSION

Alternative immersions of FTO substrates in pH = 2 TiO_2 and pH = 10 WO_3 sols result in the deposition of homogeneous films due to the electrostatic interaction between the positively TiO_2 charged nanoparticles and the negatively WO_3 charged ones. The film thickness was 400 ± 20 nm after deposition of

30 bilayers. XRD analyses carried out after the thermal treatment at 450 °C (Figure 1) evidence the presence of

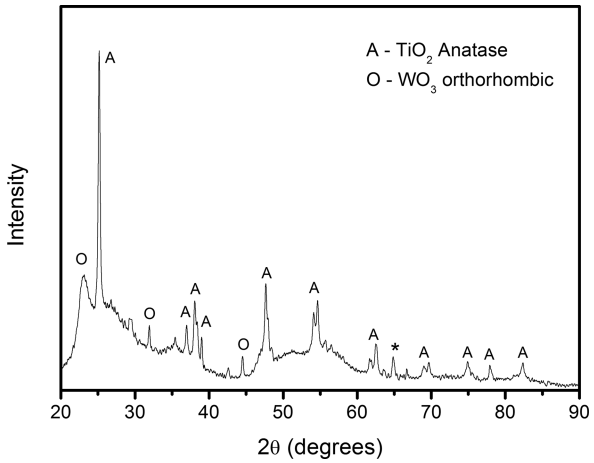

Figure 1. XRD pattern of an LbL TiO_2/WO_3 film (30 bilayers) sintered at 450 °C. The FTO diffraction peak is indicated by an asterisk (*).

anatase TiO_2. It is also observed that three weak peaks appear at $2\theta \cong 23$, 32, and 44°, tentatively assigned to the orthorhombic WO_3 (JCPDS 20-1324). Such an assignment is corroborated by previous studies carried out by Ramana et al.[51] on phase transitions in WO_3 thin films, which showed that thermal treatments between 350−500 °C favored the formation of the orthorhombic WO_3 phase. Diffraction peaks from the Na_2WO_4 precursor were not observed. The film structure was also evaluated by Raman spectroscopy (Figure 2). The

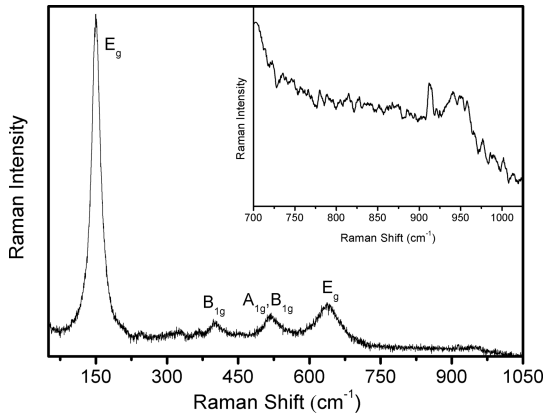

Figure 2. Raman spectrum of LbL TiO_2/WO_3 films (30 bilayers) after sintering at 450 °C.

spectrum exhibits bands characteristic to anatase TiO_2 vibration modes.[52−54] A relatively weak signal (Figure 2, inset) at ∼950 cm^{-1} corresponds to the stretching mode of terminal W═O bond and is typically observed in amorphous WO_3 samples.[55]

X-ray photoelectron spectroscopy (XPS) confirms the presence of Ti(IV) and W(VI) ions at FTO surface, Figure 3. Typical doublet Ti 2p peaks at 458.5 and 464.2 eV (Figure 3, inset) are observed and are characteristic to anatase phase.[2] The presence of WO_3 is confirmed by the appearance of peaks at 580.5 eV (W 4s), 248.5 and 260.5 eV (doublet W 4d), and 34.8 eV (W 4f).[56] The calculated W(VI)/Ti(IV) atomic ratio is 0.05, which reveals a higher concentration of TiO_2 nanoparticles in

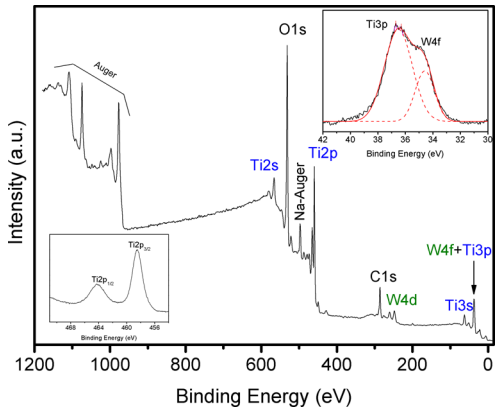

Figure 3. XPS spectrum of 30 TiO_2/WO_3 bilayers on FTO. (Inset, bottom) High-resolution spectra showing the Ti 2p peaks and (inset, top) the deconvolution of Ti 3p and W 4f signals.

the film surface and partially explains the low intensity observed for WO_3 diffraction peaks. Additional evidence for the higher TiO_2 content in the films is given by probing the thickness increments after deposition of each material (Figure S1, Supporting Information). Higher increments in thickness can be observed after deposition of TiO_2 layers.

A possible reason for the low W(VI)/Ti(IV) atomic ratio of the as-prepared TiO_2/WO_3 films is the pH employed during the LbL assembly. Dissolution of Na_2WO_4 under alkaline conditions should yield several tungsten oxyanions such as WO_6^{6-}, $W_2O_7^{2-}$, depending on the initial WO_4^{2-} concentration.[57] Only a small amount of these highly charged species needs to be adsorbed by the positively charged TiO_2 layer on FTO in order to reach the charge equilibrium\inversion at each deposition cycle. As a result, the concentration of tungsten species in the film is lower than that of the TiO_2 film. The thermal treatment performed after deposition ensures the conversion of all tungsten species in WO_3. The control of structure and composition by the pH employed during the deposition has been shown before for LbL TiO_2/SiO_2 films[58] and is an elegant manner to tune the properties of LbL metal oxide films.

The morphology of TiO_2/WO_3 film was evaluated by FESEM and AFM, Figure 4. One can observe that the film is very homogeneous, nanoporous, and composed by aggregates of spherical nanoparticles smaller than 20 nm. Its surface is relatively flat with RMS roughness of ca. 30 nm.

The deposition of 30 LbL TiO_2/WO_3 or TiO_2/TiO_2 bilayers results in a decrease of ca. 30% in the optical transmittance of the substrate in the visible region, Figure 5a. Visually, the films are translucent (Figure 5a, inset), and therefore, the decrease in the transmittance can be due light scattering or multiple reflections caused by the nanoparticle network. On the basis of the available data, it is not possible to differentiate these processes. Absorption spectrum of the TiO_2/WO_3 film, Figure 5b, evidence the presence of a shoulder at ca. 380−400 nm that is not present in pure TiO_2 films. This absorption feature can be correlated to the electronic population of WO_3 conduction band, which is expected to be approximately 0.4−0.6 eV more positive than that of anatase TiO_2.[30,39] Indirect band gap energies estimated from Tauc plots are 3.0 and 2.5 eV for pure TiO_2 and TiO_2/WO_3 films, respectively (Figure 5b, inset).

The electronic structure of the TiO_2/WO_3 films was also investigated by ultraviolet photoemission spectroscopy (UPS)

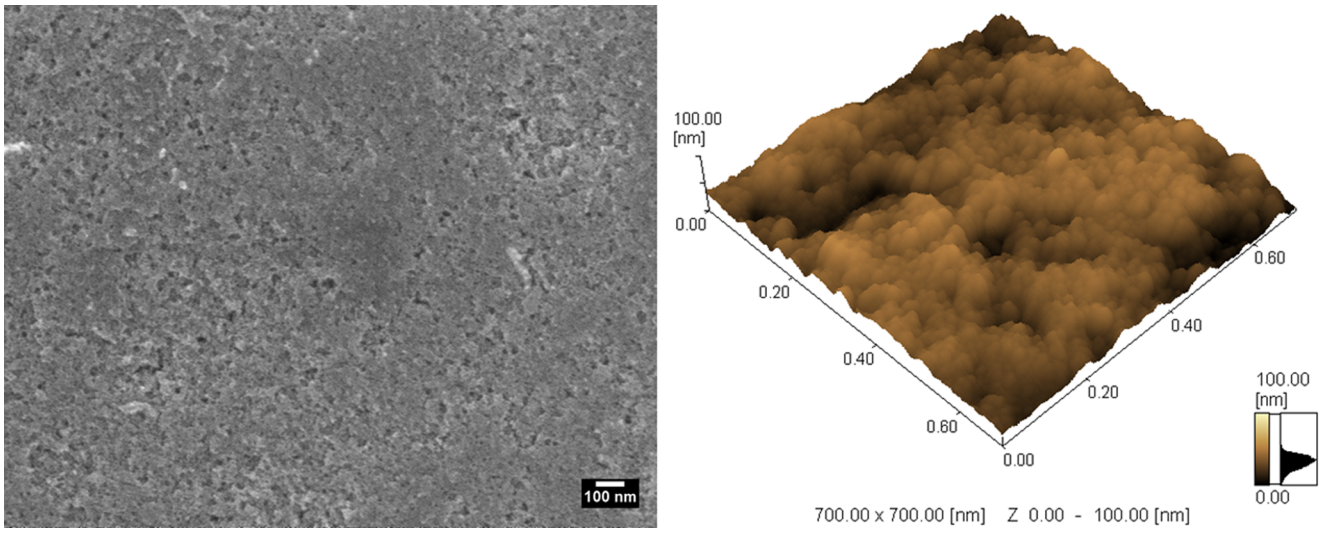

Figure 4. (Left) SEM and (right) AFM images of 30 TiO_2/WO_3 bilayers deposited over FTO substrates.

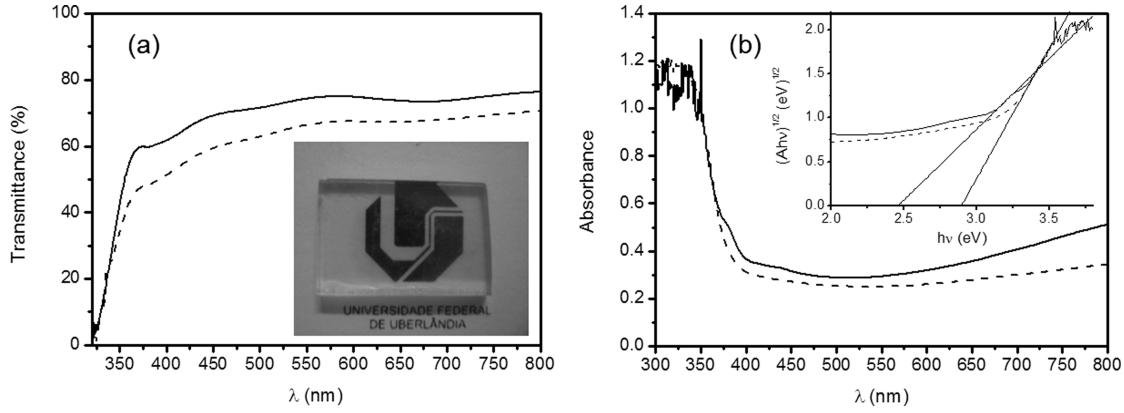

Figure 5. (a) Transmittance spectra of 30 (solid line) TiO_2/WO_3 or (dashed line) TiO_2/TiO_2 bilayers deposited on FTO and (inset) photograph of a TiO_2/WO_3 film. (b) Diffuse reflectance spectra of the films along with Tauc plots used to determine the indirect optical band gaps.

and compared to pure TiO_2 LbL films, Figure 6. One can observe that the valence band maximum remains the same for both films (at ca. 3.5 eV). Both spectra exhibit peaks at ca. 8 and 6 eV, which correspond to photoemissions from σ and π^* O 2p orbitals, respectively.[59,60] The spectrum of TiO_2/WO_3 film exhibits an increased photoemission intensity in the region around 4−6 eV. The difference between the TiO_2/WO_3 spectrum and the TiO_2/TiO_2 one results in a well-defined peak in this region that can be correlated to contribution of W_{5d} orbitals to valence band, accordingly to previous UPS studies.[61,62] Thus, diffuse reflectance measurements along with UPS allow us to conclude that, in the TiO_2/WO_3 films, the valence band maximum remains almost unchanged in relation to pure LbL TiO_2 films, and the WO_3 conduction band introduces new low lying electronic levels in relation to the conduction band of TiO_2.

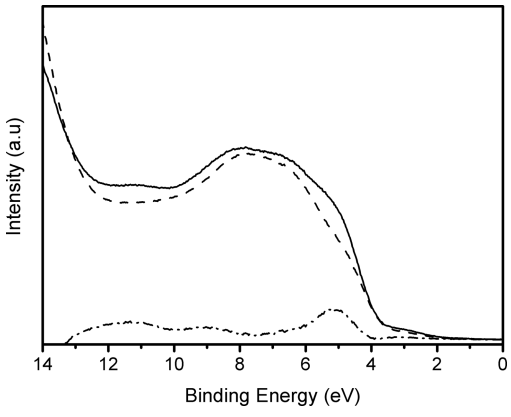

Figure 6. He 1 UPS spectra of (solid line) TiO_2/WO_3 and (dashed line) TiO_2/TiO_2 films, along with (dashed-dotted line) the difference between the two spectra.

The wettability of the LbL films deposited on FTO was evaluated by water contact angle (C.A.) measurements carried out before and after 30 min of UV(A) irradiation (Table 1). Both TiO_2/TiO_2 and TiO_2/WO_3 LbL films exhibit very low water contact angles in comparison to bare FTO (C.A. = 69°) even before UV irradiation. On the basis of the particle size of the oxides and the nanoporous morphology of LbL films, the hydrophilic behavior is probably associated with the so-called nanowicking effect, described by Rubner and co-workers,[63] in which water rapidly infiltrates through the 3D nanoporous network created by the LbL assembly.

Moreover, UV(A) irradiation of both TiO_2/WO_3 and TiO_2/TiO_2 LbL films leads to an enhancement of the surface wettability (Figure 7, Table 1). This superhydrophilic state

Table 1. Water Contact Angle Measurements for TiO_2/WO_3 and TiO_2/TiO_2 Films (30 Bilayers) Deposited over FTO Substrates

substrate	water contact angle (deg)	
	before UV(A) irradiation[a]	after UV(A) irradiation
bare FTO	69 ± 3	69 ± 3
TiO_2/WO_3	9 ± 1	<5
TiO_2/TiO_2	12 ± 2	<5

[a]Images from the C.A. measurements before irradiation are presented in Figure S2 (Supporting Information).

(C.A. <5°) observed for the LbL metal oxide films persisted for more than 96 h after storage in the dark at ambient atmosphere.

The photocatalytic properties of LbL TiO_2/WO_3 films were evaluated toward gaseous acetaldehyde oxidation under UV(A) irradiation (Figure 8). Two initial CH_3CHO concentrations (1 and 5 ppm) were employed in the photocatalytic tests. After reaching initial equilibration of the inlet flux in the dark, the system was exposed to 1 mW cm^{-2} UV(A) irradiation, and the CH_3CHO concentration started to decrease until it reached a plateau. As can be seen in Figure 8 and Table 2, the TiO_2/WO_3 LbL films are ~2 times more efficient than the films produced only with TiO_2 nanoparticles for $[CH_3CHO]_0$ = 1 ppm.

Photocatalytic oxidation of acetaldehyde mediated by metal oxide semiconductors involves its adsorption and oxidation by species such as superoxide ($O_2^{\bullet-}$) and hydroxyl radicals ($OH^{\bullet}$) produced at the semiconductor surface by the reaction of photogenerated electrons and holes with adsorbed molecular oxygen and water, respectively.[21] In the presence of the LbL metal oxides films, the photodegradation rates increase as the initial acetaldehyde concentration is enhanced from 1 to 5 ppm, Table 2. Under the irradiation condition employed in this work (~10^{19} quanta cm^{-2} s^{-1}, i.e. light-rich), this behavior can be explained by the higher diffusion/adsorption of CH_3CHO into the nanoporous structure of the films that increases the occurrence of radical chain reactions. In such reactions, photogenerated holes or $^{\bullet}OH$ radicals react with acetaldehyde to yield organic radicals able to degrade other acetaldehyde molecules.[64]

For the two acetaldehyde concentrations investigated, the LbL TiO_2/WO_3 films exhibited higher photonic efficiencies and degradation rates than those of pure self-assembled TiO_2 films. Given the similarity of the optical and morphological properties between the two films, the enhanced photocatalytic activity of the TiO_2/WO_3 assembly is directly related to its more efficient electron−hole separation. In the LbL TiO_2/WO_3 films, the self-assembly growth of the layers followed by the heating post-treatment allow the efficient interconnection between the oxide nanoparticles to yield nanoscale heterojunctions. UV(A) excitation of the films produces electron−hole pairs, and the low-lying WO_3 conduction band acts as an electron trap, while the holes are free to move within the valence bands of both oxides (Scheme 1). As a result, the electron−hole recombination rate is decreased in comparison with pure TiO_2 films, and more reacting radicals are produced at the film surface.

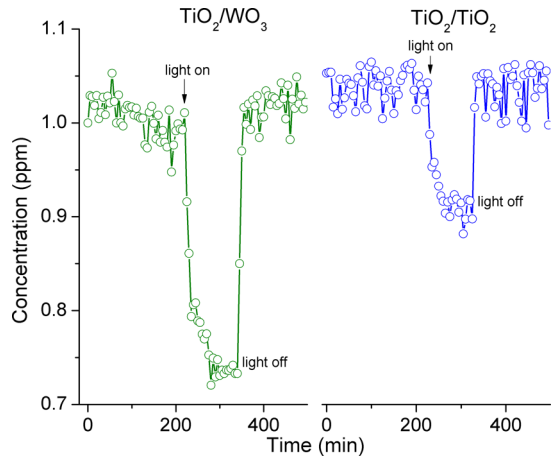

Figure 8. Time profile of the CH_3CHO photodegradation upon UV(A) irradiation (1 mW cm^{-2}) in the presence of TiO_2/WO_3 or TiO_2/TiO_2 LbL films (30 bilayers); $[CH_3CHO]_0$ = 1 ppm.

Table 2. Acetaldehyde Degradation Rates and of Photonic Efficiencies of TiO_2/WO_3 and TiO_2/TiO_2 Thin Films

thin film	$[CH_3CHO]_0$ (ppm)	degradation rate (10^{-10} mol s^{-1})	photonic efficiency, ξ (%)
TiO_2/WO_3	1.00 ± 0.02	1.7	1.5
	5.00 ± 0.05	2.8	2.3
TiO_2/TiO_2	1.00 ± 0.02	0.93	0.8
	5.00 ± 0.05	2.1	1.7
Pilkington Activ	1.00		0.94[21]

Scheme 1. Efficient Photo-Induced Electron-Hole Separation at LbL TiO_2/WO_3 Films

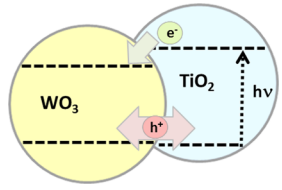

Another key aspect for the high photocatalytic activity of LbL TiO_2/WO_3 film, in contrast to the pure TiO_2 film or the commercially available Pilkington Active glass, is the low W(VI)/Ti(IV) ratio. It is well-known that TiO_2/WO_3 heterostructures with high tungsten contents exhibit low catalytic activity due to the occurrence of photochromism.[36,39] This phenomenon is related to electron accumulation at the WO_3 conduction band, which is enhanced in highly crystalline microsized particles. The occurrence of photochromism is

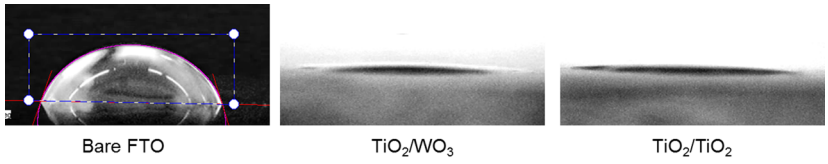

Figure 7. Water contact angle measurements of bare and modified FTO surfaces after 30 min of UV(A) treatment.

deleterious for the photocatalytic activity because the WO_3 conduction band is too positive to reduce O_2 to superoxide radicals ($O_2^{\bullet-}$). Moreover, the accumulated electrons can react with $^{\bullet}OH$ radicals to yield OH^- anions.

No photochromism was observed in the LbL TiO_2/WO_3 films, which means electron accumulation in the WO_3 conduction band is limited, probably by the low W(VI) content of the film and by its nanosized heterostructure. A similar effect has been reported by Yang et al. for TiO_2/WO_3 composites with different WO_3 contents.[39] The authors have observed better photocatalytic activities for low W(VI)/Ti(IV) ratios. Thus, photoexcitation of LbL TiO_2/WO_3 films should be followed by electron transfer from TiO_2 to WO_3 nanoparticles, which decreases the charge recombination, allowing the production of more $^{\bullet}OH$ radicals by the reaction of holes with adsorbed water and improving the photocatalytic activity. The adequate W(VI)/Ti(IV) ratio along with the nanosized particles promote more efficient charge separation than in pure LbL TiO_2 films, without the occurrence of photochromism.

Visible-light photoactivity of TiO_2/WO_3 films was evaluated using a 420 nm LED source (1 mW cm^{-2}), however no degradation of acetaldehyde was observed. This behavior may be associated with the low light absorption in the irradiation wavelength of such thin films. The UV(A) photocatalytic activity of LbL TiO_2/WO_3 films on FTO is higher than that of commercial photoactive glasses, such as Pilkington Activ or platinum/titania composite films,[21] and therefore, they represent a cost-effective solution for production of self-cleaning photocatalytic surfaces. Additionally, the LbL films exhibit superhydrophilicity under UV(A) irradiation, which is a desired property for self-cleaning surfaces.

CONCLUSIONS

The layer-by-layer technique was successfully applied to produce new TiO_2/WO_3 thin films with enhanced photocatalytic activity. The films were produced by alternative immersions of the substrates into sols of TiO_2 (pH = 2) and WO_3 (pH = 10) nanoparticles, leading to the production of films with low W(VI)/Ti(IV) molar ratio. The photocatalytic activity of the films was evaluated against gaseous acetaldehyde degradation, and the determined photonic efficiencies are higher than those of pure LbL TiO_2 films or Pilkington Activ glass. The results show the role of WO_3 nanoparticles as efficient electron traps able to decrease the electron−hole recombination rate. The small particle size employed in the self-assembly deposition leads to formation of highly homogeneous films constituted by nanoscale heterojunctions responsible for the efficient charge separation. The relatively high photocatalytic activity along with the good optical properties and (super)hydrophilicity make such films suitable for applications such as self-cleaning surfaces in windows, roofs, walls and so on.

ASSOCIATED CONTENT

Supporting Information

Plot of the TiO_2/WO_3 film thickness increment after deposition of TiO_2 or WO_3 layer and images of water contact angle measurements on LbL films before UV(A) irradiation. This material is available free of charge via the Internet at http://pubs.acs.org.

AUTHOR INFORMATION

Corresponding Authors

*E-mail: otaviopatrocinio@iqufu.ufu.br.

*E-mail: bahnemann@iftc.uni-hannover.de.

Notes

The authors declare no competing financial interest.

ACKNOWLEDGMENTS

This work was supported by Fundação de Amparo à Pesquisa do Estado de Minas Gerais (FAPEMIG), Conselho Nacional de Desenvolvimento Científico e Tecnológico (CNPq) and Coordenação de Aperfeiçoamento de Pessoal de Nível Superior (CAPES). AOTP is thankful to Dr. André S. Polo for the thickness measurements, Dr. Newton M. Barbosa Neto and the Physics Postgraduation Program of Universidade Federal do Pará for the Raman spectra, and the DLR Green Talents program for the research stay in Germany. Financial support by the Deutsche Forschungsgemeinschaft (DFG) for JF is gratefully acknowledged (Project Number BA 1137/8-2).

REFERENCES

(1) Zhang, L.; Dillert, R.; Bahnemann, D.; Vormoor, M. Photo-Induced Hydrophilicity and Self-Cleaning: Models and Reality. *Energy Environ. Sci.* **2012**, *5*, 7491−7507.

(2) Xi, B.; Verma, L. K.; Li, J.; Bhatia, C. S.; Danner, A. J.; Yang, H.; Zeng, H. C. TiO_2 Thin Films Prepared Via Adsorptive Self-Assembly for Self-Cleaning Applications. *ACS Appl. Mater. Interfaces* **2012**, *4*, 1093−1102.

(3) Lai, Y.; Tang, Y.; Gong, J.; Gong, D.; Chi, L.; Lin, C.; Chen, Z. Transparent Superhydrophobic/Superhydrophilic TiO_2-Based Coatings for Self-Cleaning and Anti-Fogging. *J. Mater. Chem.* **2012**, *22*, 7420−7426.

(4) Cai, J.; Ye, J.; Chen, S.; Zhao, X.; Zhang, D.; Chen, S.; Ma, Y.; Jin, S.; Qi, L. Self-Cleaning, Broadband and Quasi-Omnidirectional Antireflective Structures Based on Mesocrystalline Rutile TiO_2 Nanorod Arrays. *Energy Environ. Sci.* **2012**, *5*, 7575−7581.

(5) Ganesh, V. A.; Raut, H. K.; Nair, A. S.; Ramakrishna, S. A Review on Self-Cleaning Coatings. *J. Mater. Chem.* **2011**, *21*, 16304−16322.

(6) Peruchon, L.; Puzenat, E.; Herrmann, J. M.; Guillard, C. Photocatalytic Efficiencies of Self-Cleaning Glasses. Influence of Physical Factors. *Photochem. Photobiol. Sci.* **2009**, *8*, 1040−1046.

(7) Tuteja, A.; Choi, W. J.; McKinley, G. H.; Cohen, R. E.; Rubner, M. F. Design Parameters for Superhydrophobicity and Superoleophobicity. *MRS Bull.* **2008**, *33*, 752−758.

(8) Fujishima, A.; Zhang, X.; Tryk, D. A. TiO_2 Photocatalysis and Related Surface Phenomena. *Surf. Sci. Rep.* **2008**, *63*, 515−582.

(9) Euvananont, C.; Junin, C.; Inpor, K.; Limthongkul, P.; Thanachayanont, C. TiO_2 Optical Coating Layers for Self-Cleaning Applications. *Ceram. Int.* **2008**, *34*, 1067−1071.

(10) Mills, A.; McFarlane, M. Current and Possible Future Methods of Assessing the Activities of Photocatalyst Films. *Catal. Today* **2007**, *129*, 22−28.

(11) Wang, R.; Hashimoto, K.; Fujishima, A.; Chikuni, M.; Kojima, E.; Kitamura, A.; Shimohigoshi, M.; Watanabe, T. Light-Induced Amphiphilic Surfaces. *Nature* **1997**, *388*, 431−432.

(12) Cedillo-González, E. I.; Riccò, R.; Montorsi, M.; Montorsi, M.; Falcaro, P.; Siligardi, C. Self-Cleaning Glass Prepared from a Commercial TiO_2 Nano-Dispersion and Its Photocatalytic Performance under Common Anthropogenic and Atmospheric Factors. *Build. Environ.* **2014**, *71*, 7−14.

(13) Rahal, R.; Pigot, T.; Foix, D.; Lacombe, S. Photocatalytic Efficiency and Self-Cleaning Properties under Visible Light of Cotton Fabrics Coated with Sensitized TiO_2. *Appl. Catal., B* **2011**, *104*, 361−372.

(14) Mellott, N. P.; Durucan, C.; Pantano, C. G.; Guglielmi, M. Commercial and Laboratory Prepared Titanium Dioxide Thin Films

for Self-Cleaning Glasses: Photocatalytic Performance and Chemical Durability. *Thin Solid Films* **2006**, *502*, 112−120.
(15) Parkin, I. P.; Palgrave, R. G. Self-Cleaning Coatings. *J. Mater. Chem.* **2005**, *15*, 1689−1695.
(16) Mehrjouei, M.; Müller, S.; Möller, D. Degradation of Oxalic Acid in a Photocatalytic Ozonation System by Means of Pilkington Active Glass. *J. Photochem. Photobiol. A* **2011**, *217*, 417−424.
(17) Chin, P.; Ollis, D. F. Decolorization of Organic Dyes on Pilkington Activ Photocatalytic Glass. *Catal. Today* **2007**, *123*, 177−188.
(18) Mills, A.; Lepre, A.; Elliott, N.; Bhopal, S.; Parkin, I. P.; O'Neill, S. A. Characterisation of the Photocatalyst Pilkington Activ: A Reference Film Photocatalyst? *J. Photochem. Photobiol. A* **2003**, *160*, 213−224.
(19) Wu, M.; Yu, H.; Xu, M. A Preliminary Research on V/N−TiO_2 Self-Cleaning Thin Film by Sol−Gel Method under the Guidance of First Principle Method Density Functional Theory (DFT). *Appl. Catal., B* **2013**, *129*, 351−366.
(20) Asahi, R.; Morikawa, T.; Ohwaki, T.; Aoki, K.; Taga, Y. Visible-Light Photocatalysis in Nitrogen-Doped Titanium Oxides. *Science* **2001**, *293*, 269−271.
(21) Ismail, A. A.; Bahnemann, D. W.; Rathousky, J.; Yarovyi, V.; Wark, M. Multilayered Ordered Mesoporous Platinum/Titania Composite Films: Does the Photocatalytic Activity Benefit from the Film Thickness? *J. Mater. Chem.* **2011**, *21*, 7802−7810.
(22) Ismail, A. A.; Bahnemann, D. W. One-Step Synthesis of Mesoporous Platinum/Titania Nanocomposites as Photocatalyst with Enhanced Photocatalytic Activity for Methanol Oxidation. *Green Chem.* **2011**, *13*, 428−435.
(23) Ismail, A. A.; Bahnemann, D. W. Metal-Free Porphyrin-Sensitized Mesoporous Titania Films for Visible-Light Indoor Air Oxidation. *ChemSusChem* **2010**, *3*, 1057−1062.
(24) Fateh, R.; Dillert, R.; Bahnemann, D. Self-Cleaning Properties, Mechanical Stability, and Adhesion Strength of Transparent Photocatalytic TiO_2-ZnO Coatings on Polycarbonate. *ACS Appl. Mater. Interfaces* **2014**, *6*, 2269−2277.
(25) Pinho, L.; Mosquera, M. J. Photocatalytic Activity of TiO_2−SiO_2 Nanocomposites Applied to Buildings: Influence of Particle Size and Loading. *Appl. Catal., B* **2013**, *134−135*, 205−221.
(26) Li, X.; He, J. Synthesis of Raspberry-Like SiO_2-TiO_2 Nanoparticles toward Antireflective and Self-Cleaning Coatings. *ACS Appl. Mater. Interfaces* **2013**, *5*, 5282−5290.
(27) Wu, Z.; Lee, D.; Rubner, M. F.; Cohen, R. E. Structural Color in Porous, Superhydrophilic, and Self-Cleaning SiO_2/TiO_2 Bragg Stacks. *Small* **2007**, *3*, 1445−1451.
(28) Miyauchi, M.; Nakajima, A.; Fujishima, A.; Hashimoto, K.; Watanabe, T. Photoinduced Surface Reactions on TiO_2 and $SrTiO_3$ Films: Photocatalytic Oxidation and Photoinduced Hydrophilicity. *Chem. Mater.* **2000**, *12*, 3−5.
(29) Ismail, A. A.; Robben, L.; Bahnemann, D. W. Study of the Efficiency of UV and Visible-Light Photocatalytic Oxidation of Methanol on Mesoporous RuO_2-TiO_2 Nanocomposites. *ChemPhysChem* **2011**, *12*, 982−991.
(30) Miyauchi, M.; Nakajima, A.; Hashimoto, K.; Watanabe, T. A Highly Hydrophilic Thin Film under 1 $\mu w/cm^2$ UV Illumination. *Adv. Mater.* **2000**, *12*, 1923−1927.
(31) Djaoued, Y.; Balaji, S.; Beaudoin, N. Sol−Gel Synthesis of Mesoporous WO_3-TiO_2 Composite Thin Films for Photochromic Devices. *J. Sol−Gel Sci. Technol.* **2013**, *65*, 374−383.
(32) Zhu, Y.; Su, X.; Yang, C.; Gao, X.; Xiao, F.; Wang, J. Synthesis of TiO_2-WO_3 Nanocomposites as Highly Sensitive Benzene Sensors and High-Efficiency Adsorbents. *J. Mater. Chem.* **2012**, *22*, 13914−13917.
(33) Park, H.; Bak, A.; Jeon, T. H.; Kim, S.; Choi, W. Photo-Chargeable and Dischargeable TiO_2 and WO_3 Heterojunction Electrodes. *Appl. Catal., B* **2012**, *115*, 74−80.
(34) Li, Y.; Hsu, P.-C.; Chen, S.-M. Multi-Functionalized Biosensor at WO_3-TiO_2 Modified Electrode for Photoelectrocatalysis of Norepinephrine and Riboflavin. *Sens. Actuators, B* **2012**, *174*, 427−435.
(35) Depero, L. E.; Ferroni, M.; Guidi, V.; Marca, G.; Martinelli, G.; Nelli, P.; Sangaletti, L.; Sberveglieri, G. Preparation and Micro-Structural Characterization of Nanosized Thin Film of TiO_2 -WO_3 as a Novel Material with High Sensitivity Towards NO_2. *Sens. Actuators, B* **1996**, *36*, 381−383.
(36) Riboni, F.; Bettini, L. G.; Bahnemann, D. W.; Selli, E. WO_3-Tio_2 vs TiO_2 Photocatalysts: Effect of the W Precursor and Amount on the Photocatalytic Activity of Mixed Oxides. *Catal. Today* **2013**, *209*, 28−34.
(37) Cheng, P.; Deng, C. S.; Liu, D. N.; Dai, X. M. Titania Surface Modification and Photovoltaic Characteristics with Tungsten Oxide. *Appl. Surf. Sci.* **2008**, *254*, 3391−3396.
(38) Depero, L. E.; Groppelli, S.; NataliSora, I.; Sangaletti, L.; Sberveglieri, G.; Tondello, E. Structural Studies of Tungsten-Titanium Oxide Thin Films. *J. Solid State Chem.* **1996**, *121*, 379−387.
(39) Yang, J.; Zhang, X.; Liu, H.; Wang, C.; Liu, S.; Sun, P.; Wang, L.; Liu, Y. Heterostructured TiO_2/WO_3 Porous Microspheres: Preparation, Characterization, and Photocatalytic Properties. *Catal. Today* **2013**, *201*, 195−202.
(40) Irie, H.; Mori, H.; Hashimoto, K. Interfacial Structure Dependence of Layered TiO_2/WO_3 Thin Films on the Photoinduced Hydrophilic Property. *Vacuum* **2004**, *74*, 625−629.
(41) Patrocinio, A. O. T.; Paterno, L. G.; Murakami Iha, N. Y. Role of Polyelectrolyte for Layer-by-Layer Compact TiO_2 Films in Efficiency Enhanced Dye-Sensitized Solar Cells. *J. Phys. Chem. C* **2010**, *114*, 17954−17959.
(42) Paula, L. F.; Amaral, R. C.; Murakami Iha, N. Y.; Paniago, R. M.; Machado, A. E. H.; Patrocinio, A. O. T. New Layer-by-Layer Nb_2O_5−TiO_2 Film as an Effective Underlayer in Dye-Sensitised Solar Cells. *RSC Adv.* **2014**, *4*, 10310−10316.
(43) Yuan, S.; Mu, J.; Mao, R.; Li, Y.; Zhang, Q.; Wang, H. All-Nanoparticle Self-Assembly ZnO/TiO_2 Heterojunction Thin Films with Remarkably Enhanced Photoelectrochemical Activity. *ACS Appl. Mater. Interfaces* **2014**, *6*, 5719−5725.
(44) Cohen, R. E.; Shimomura, H.; Gemici, Z.; Rubner, M. F. Layer-by-Layer-Assembled High-Performance Broadband Antireflection Coatings. *ACS Appl. Mater. Interfaces* **2010**, *2*, 813−820.
(45) Lee, D.; Rubner, M. F.; Cohen, R. E. All-Nanoparticle Thin-Film Coatings. *Nano Lett.* **2006**, *6*, 2305−2312.
(46) Test Method for Air-Purification Performance of Semiconducting Photocatalytic Materials—Part 2: Removal of Acetaldehyde, ISO 22197-2:2011. International Organization for Standardization: Geneva, Switzerland, 2011.
(47) Kim, H.; Choi, W. Effects of Surface Fluorination of TiO_2 on Photocatalytic Oxidation of Gaseous Acetaldehyde. *Appl. Catal., B* **2007**, *69*, 127−132.
(48) Patrocínio, A. O. T.; Paniago, E. B.; Paniago, R. M.; Murakami Iha, N. Y. XPS Characterization of Sensitized *n*-TiO_2 Thin Films for Dye-Sensitized Solar Cell Applications. *Appl. Surf. Sci.* **2008**, *254*, 1874−1879.
(49) Patrocinio, A. O. T.; El-Bacha, A. S.; Paniago, E. B.; Paniago, R. M.; Murakami Iha, N. Y. Influence of the Sol−Gel Ph Process and Compact Film on the Efficiency of TiO_2-Based Dye-Sensitized Solar Cells. *Int. J. Photoenergy* **2012**, *638571*, 1−7.
(50) Ismail, A. A.; Bahnemann, D. W. Pt Colloidal Accommodated into Mesoporous TiO_2 Films for Photooxidation of Acetaldehyde in Gas Phase. *Chem. Eng. J.* **2012**, *203*, 174−181.
(51) Ramana, C. V.; Utsunomiya, S.; Ewing, R. C.; Julien, c. M.; Becker, U. Structural Stability and Phase Transitions in WO_3 Thin Films. *J. Phys. Chem. B* **2006**, *110*, 10430−10435.
(52) Zhang, W. F.; He, Y. L.; Zhang, M. S.; Yin, Z.; Chen, Q. Raman Scattering Study on Anatase Tio_2 Nanocrystals. *J. Phys. D: Appl. Phys.* **2000**, *33*, 912.
(53) Ohsaka, T. Temperature Dependence of the Raman Spectrum in Anatase TiO_2. *J. Phys. Soc. Jpn.* **1980**, *48*, 1661−1668.
(54) Georgescu, D.; Baia, L.; Ersen, O.; Baia, M.; Simon, S. Experimental Assessment of the Phonon Confinement in TiO_2 Anatase Nanocrystallites by Raman Spectroscopy. *J. Raman Spectrosc.* **2012**, *43*, 876−883.

(55) Santato, C.; Odziemkowski, M.; Ulmann, M.; Augustynski, J. Crystallographically Oriented Mesoporous WO_3 Films: Synthesis, Characterization, and Applications. *J. Am. Chem. Soc.* **2001**, *123*, 10639−10649.
(56) Weinhardt, L.; Blum, M.; Baer, M.; Heske, C.; Cole, B.; Marsen, B.; Miller, E. L. Electronic Surface Level Positions of WO_3 Thin Films for Photoelectrochemical Hydrogen Production. *J. Phys. Chem. C* **2008**, *112*, 3078−3082.
(57) Barré, T.; Arurault, L.; Sauvage, F. X. Chemical Behavior of Tungstate Solutions: Part 1. A Spectroscopic Survey of the Species Involved. *Spectrochim. Acta, Part A* **2005**, *61*, 551−557.
(58) Lee, D.; Omolade, D.; Cohen, R. E.; Rubner, M. F. Ph-Dependent Structure and Properties of TiO_2/SiO_2 Nanoparticle Multilayer Thin Films. *Chem. Mater.* **2007**, *19*, 1427−1433.
(59) Orendorz, A.; Wusten, J.; Ziegler, C.; Gnaser, H. Photoelectron Spectroscopy of Nanocrystalline Anatase TiO_2 Films. *Appl. Surf. Sci.* **2005**, *252*, 85−88.
(60) Sanjinés, R.; Tang, H.; Berger, H.; Gozzo, F.; Margaritondo, G.; Lévy, F. Electronic Structure of Anatase TiO_2 Oxide. *J. Appl. Phys.* **1994**, *75*, 2945−2951.
(61) Bussolotti, F.; Lozzi, L.; Passacantando, M.; La Rosa, S.; Santucci, S.; Ottaviano, L. Surface Electronic Properties of Polycrystalline WO_3 Thin Films: A Study by Core Level and Valence Band Photoemission. *Surf. Sci.* **2003**, *538*, 113−123.
(62) Bullett, D. W. Bulk and Surface Electron-States in WO_3 and Tungsten Bronzes. *J. Phys. C: Solid State Phys.* **1983**, *16*, 2197−2207.
(63) Cebeci, F. C.; Wu, Z. Z.; Zhai, L.; Cohen, R. E.; Rubner, M. F. Nanoporosity-Driven Superhydrophilicity: A Means to Create Multifunctional Antifogging Coatings. *Langmuir* **2006**, *22*, 2856−2862.
(64) Ohko, Y.; Tryk, D. A.; Hashimoto, K.; Fujishima, A. Autooxidation of Acetaldehyde Initiated by TiO_2 Photocatalysis under Weak UV Illumination. *J. Phys. Chem. B* **1998**, *102*, 2699−2704.